Journal of Cancer Research and Clinical Oncology (2019) 145:615–623
https://doi.org/10.1007/s00432-018-2815-1

ORIGINAL ARTICLE – CANCER RESEARCH

T-cell receptor-α CDR3 domain chemical features correlate with survival rates in bladder cancer

Boris I. Chobrutskiy[1] · Saif Zaman[1] · Andrea Diviney[1] · Moody M. Mihyu[1] · George Blanck[1,2]

Received: 20 October 2018 / Accepted: 4 December 2018 / Published online: 11 December 2018

Abstract

Purpose In certain cancer settings, a T-cell response to cancer represents a relatively favorable outcome. Thus, the near-future challenges include a better understanding of exactly which T-cell features contribute to a response to which cancer antigen-groups, to maximize the opportunities for tumor-infiltrating lymphocyte (TIL)-based therapies and other immunotherapies.
Methods The immune receptor complementarity determining region-3 (CDR3) is considered to be important for antigen binding, hence, in this report, we evaluated the chemical features of the CDR3 of 846 T-cell receptor-α (TCR-α) coding regions associated with bladder tumor tissue, using bioinformatics databases.
Results Results indicated that statistically significantly distinct, low value, CDR3 region isoelectric points associate with a better outcome (log rank $p < 0.027$, overall survival). Moreover, in samples representing the more favorable isoelectric points, known driver mutations, for example, PIK3CA (E → K) with chemically complementary features overlap the better-outcome, low isoelectric point samples. Further work extended these results, i.e., survival rate-CDR3 associations, to other CDR3 chemical features and other cancers, consistent with the initial isoelectric point-related, bladder cancer findings.
Conclusions A bioinformatics assessment of cancer-associated TCR biochemical features may improve the accuracy of the predictions of which TILs will be best for ex-vivo amplification and which patients will benefit from other immunotherapies.

Keywords T-cell receptor-alpha CDR3 · Biochemical features · Cancer survival outcomes · Bioinformatics · Antigen chemical complementarity

Abbreviations

BLCA	Bladder cancer
CDR3	Complementarity determining region-3
DFS	Disease-free survival
ESCA	Esophageal carcinoma
NCPR	Net charge per residue
OS	Overall survival
OVCA	Ovarian cancer
STAD	Stomach adenocarcinoma
TCR	T-cell receptor
TCGA	The cancer genome atlas
TILs	Tumor-infiltrating lymphocytes
WXS	Whole exome sequence

✉ George Blanck
gblanck@health.usf.edu

[1] Department of Molecular Medicine, Morsani College of Medicine, University of South Florida, Tampa, USA

[2] Immunology Program, H. Lee Moffitt Cancer Center and Research Institute, 12901 Bruce B. Downs Bd. MDC7, Tampa, FL 33612, USA

Introduction

Many studies have supported the conclusion that bladder cancer patients with a T-cell infiltrate have a better prognosis (el-Demiry et al. 1987; Prescott et al. 1989; Chen et al. 2000; Parodi et al. 2016; Samy et al. 2017; Stober 1978), although bladder cancer recurrence can be associated with an over-abundance of regulatory T-cells (Parodi et al. 2016). In a variety of other cancers, there have been similar conclusions, with melanoma generally representing the greatest advances with regard to identification of naturally occurring, specific TCRs against specific cancer antigens; and CD19-positive lymphomas representing the greatest advances with common-antigen directed T-cell killing (Davila et al. 2013; Kochenderfer et al. 2015).

These successes have raised the issue of how to identify, and possibly exploit, naturally occurring T-cells that effectively recognize cancer antigens that occur in multiple patients. Such processes of identification would allow for a more consistent evaluation of patients, in the sense that it is highly unlikely that a single TCR amino acid (AA)

sequence, evidenced to have effectiveness in one patient, will have the same effectiveness in the next patient. This problem is due to two issues. First, the TCR V and J usage, and possibly the CDR3, are restricted to HLA types (Klarenbeek et al. 2015; Zeng et al. 2016; Di Sante et al. 2015), and recent work has indicated that only certain TCR V and J usage, HLA allele combinations are associated with the highest survival rates (Callahan et al. 2018). And second, effective cancer antigens, and neo-antigens, may vary from patient to patient. To a certain extent, these problems are evaded by the preparation of patient tumor-infiltrating lymphocytes (TILs) ex vivo, but this approach on a patient-to-patient basis has mixed results, with many patients expiring prior to sufficient ex-vivo replication of TILs.

Despite the above-indicated challenges to a "pre-identification" of an effective TCR sequence, patients may have HLA types in common and cancer antigens in common, supporting a careful consideration of how these commonalities might be exploited. In the case of HLA types, over many years of effort, there have been a few examples of HLA types associated with the development of certain cancers, with ref (Cheng et al. 2018) being one recent example. And as noted, it is possible detect at least preliminary indications of V and J usage associated with a distinct outcomes (Callahan et al. 2018), although there is to date no empirical evidence supporting that work. Furthermore, the statistical requirements of validating and re-validating the association of specific V and J usage, HLA allele combinations with survival rates, especially given the impracticality of establishing clinical trials with a patient cohort make-up consisting of a specific HLA allele distribution, makes it likely that progress in HLA-related prognosis or therapy design will be slow. And, the antigenic variation, from tumor to tumor, may reduce the predictive value of particular V and J usage, HLA allele combinations. In particular, in the previous studies associating V and J usage, HLA allele combinations with survival rates (Callahan et al. 2018), no consistent CDR3 feature(s) was apparent.

Thus, in this study, we considered the possibility that, although specific AA sequences of the antigen-binding CDR3 might not be repeated from patient to patient, patients with the same driver or cancer-specific mutations, could reveal CDR3 regions with common chemical features, presumably reflecting common cancer antigens. Addressing this prospect is facilitated by the relatively convenient availability of very large numbers of immune receptor recombination reads from tumor exome files, where extensive studies have firmly supported the conclusion that such immune receptor recombination reads represent TILs (Samy et al. 2017; Mai et al. 2018; Tu et al. 2017, 2018; Kinskey et al. 2018; Tong et al. 2017; Gill et al. 2016; Li et al. 2016, 2017; Iglesia et al. 2016; Brown et al. 2015). Particularly, in the case of bladder cancer, results indicated the likely usefulness of bioinformatics approaches to the assessment of CDR3 chemistry in advancing the usefulness of TCR data for patient prognosis and possibly therapy design.

Methods

Recovery of immune receptor V(D)J recombination reads

The genomic data commons (GDC) web portal (https://portal.gdc.cancer.gov/) was queried for bladder cancer (BLCA) whole exome sequence (WXS) files. Four hundred-eighteen primary tumor WXS and 394 blood WXS files were downloaded to USF research computing using the GDC data transfer tool (version 1.3). (Download manifest, Table S1). V(D)J recombination read recovery were performed in two stages: the first stage used a collection of scripts similar to previous publications (Callahan et al. 2018; Mai et al. 2018; Tu et al. 2018; Kinskey et al. 2018), and the second stage performed pairwise alignment of candidate reads to known V and J sequences. Known V and J sequences were obtained from The International Immunogenetics Information System (http://www.imgt.org/). The quantitative parameters for the pairwise alignment were: (1) nucleotide match, +5; (2) mismatch, − 10; (3) opening gap, − 10; and (4) extending gap, − 10. The threshold for a V or J gene segment match was a score greater than or equal to 65. (The original script for this process is available upon email to the corresponding author.)

Table 1 KM analyses for barcode groups of the highest versus lowest, TRA CDR3 isoelectric points, as determined by recovery of TRA recombination reads from TCGA BLCA WXS files

Tissue source of TRA recombination reads	Survival	Lowest 50% average isoelectric point	Highest 50% average isoelectric point	Isoelectric point *p* value distinction	Survival Log rank *p* value	Number of barcodes
Primary tumor	Overall	5.80	8.16	< 0.0001	0.039	224
Primary tumor	Disease-free	5.84	8.09	< 0.0001	0.020	172
Blood	Overall	6.12	8.16	< 0.0001	0.624	326
Blood	Disease-free	6.12	8.14	< 0.0001	0.347	265

The lower 50% group represented the better survival rate in the case of primary tumor

The required parameters for V(D)J recombination read identification were reads containing both a V and J region, a productive in-frame junction with no stop codons, a match length of at least 20 nucleotides for each gene segment, and at least a 90% nucleotide match fidelity. (Example list of recovery of recombination reads, Table S2).

Assessment of physico-chemical features of CDR3 regions

V(D)J recombination read CDR3 domains were identified and translated using an original script (available upon email to the corresponding author). Isoelectric point, fraction of

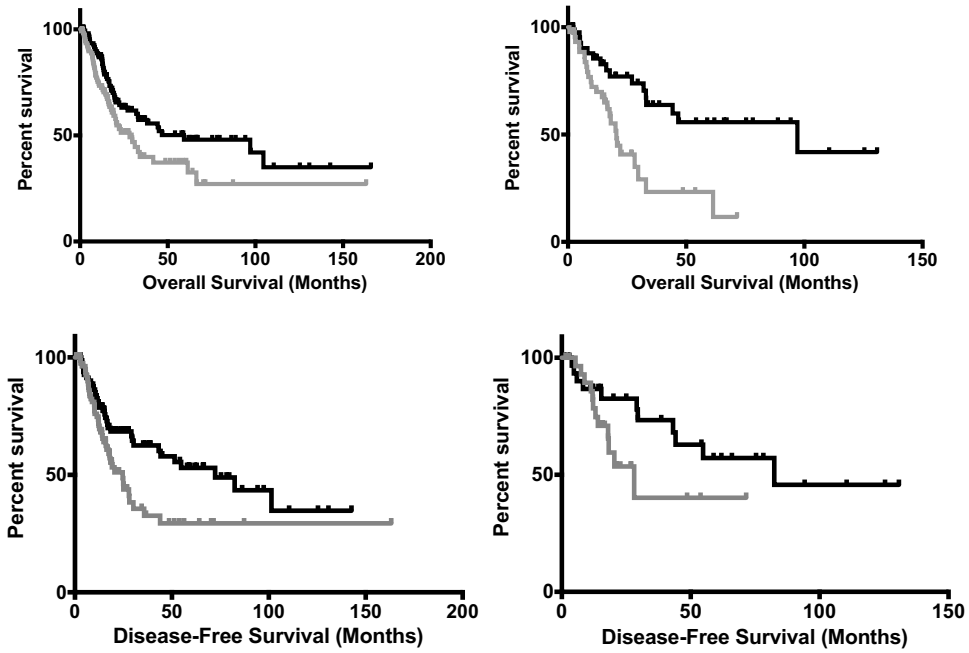

Fig. 1 Survival rates associated with TRA CDR3 isoelectric points. **a** Kaplan–Meier (KM) analysis of OS represented by TCGA BLCA barcodes representing the highest 50% (grey) and lowest 50% (black) TRA CDR3 isoelectric points (left panel); and representing the highest 20% (grey) and lowest 20% (black) TRA CDR3 isoelectric points (right panel). Median OS for highest 50% isoelectric point group, 28.22 months. Median OS for lowest 50% isoelectric point group, 59.26 months. Log rank comparison *p* value 0.0278. Median OS for highest 20% isoelectric point group, 20.47 months. Median OS for lowest 20% isoelectric point group, 97.04 months. Log rank comparison *p* value 0.0013. **b** KM analysis of DFS for BLCA barcodes representing the highest 50% (grey) compared to lowest 50% (black) of TRA CDR3 isoelectric points (left panel); and representing the highest 20% (grey) compared to lowest 20% (black) of TRA CDR3 isoelectric points (right panel). Median DFS for highest 50% isoelectric point group, 24.64 months. Median DFS for lowest 50% isoelectric point group, 72.34 months. Log rank comparison *p* value 0.0125. Median DFS for highest 20% isoelectric point group, 28.06 months. Median DFS for lowest 20% isoelectric point group, 82.42 months. Log rank comparison *p* value 0.0930

Table 2 KM analyses for highest versus lowest isoelectric point groups among barcodes with gene mutations

Gene	Mutants *p* value (overall survival)	Non-mutants *p* value (overall survival)	Mutants *p* value (disease-free survival)	Non-mutants *p* value (disease-free survival)	*n*	Average Isoelectric point change due to the mutant amino acid substitution
PIK3CA	0.055	0.095	0.009	0.642	54	+2.76
ITPR2	0.007	0.196	0.0007	0.181	26	+1.26
LAMA3	0.010	0.171	0.058	0.091	24	+1.08
NCOR1	0.030	0.165	0.007	0.088	27	+0.74
ZFHX4	0.005	0.181	0.002	0.064	27	+0.21
NEB	0.012	0.188	0.017	0.091	39	+0.17
MDN1	0.046	0.160	0.025	0.124	26	+0.12
AHNAK2	0.050	0.216	0.015	0.100	42	− 0.46

Only genes representing cases where the gene mutated set, in comparison to the gene wild-type set, showed a statistically significant survival distinction, based on isoelectric point values, are listed in this table

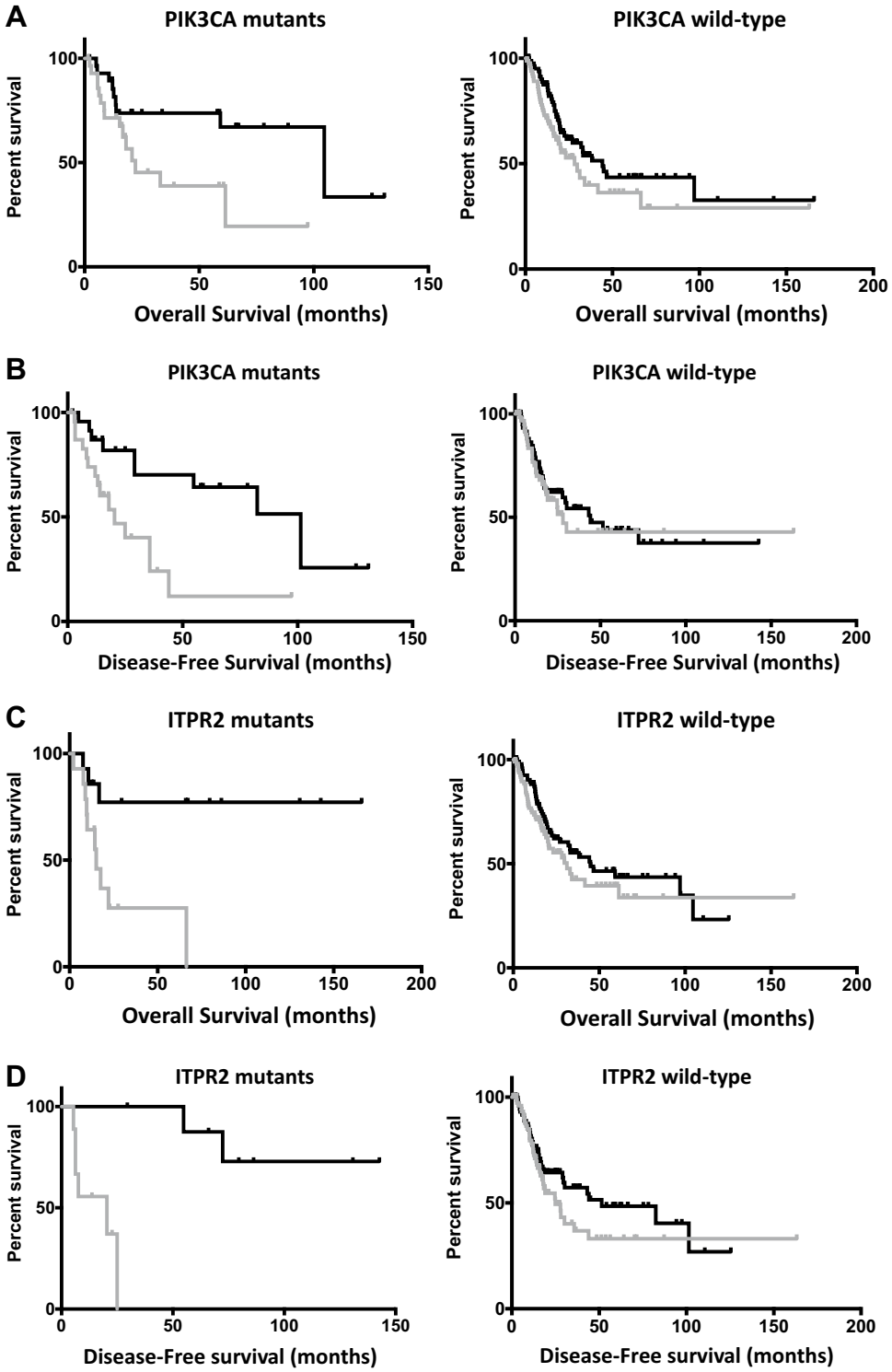
A
PIK3CA mutants
Percent survival
Overall Survival (months)
PIK3CA wild-type
Overall survival (months)
B
PIK3CA mutants
Disease-Free Survival (months)
PIK3CA wild-type
C
ITPR2 mutants
Overall Survival (months)
ITPR2 wild-type
D
ITPR2 mutants
Disease-Free survival (months)
ITPR2 wild-type

◂**Fig. 2** Survival distinctions within mutated gene groups, based on TRA CDR3 isoelectric point values. **a** KM analysis of OS for BLCA barcodes representing the highest 50% (grey) compared to the lowest 50% (black) of TRA CDR3 isoelectric points, among barcodes representing PIK3CA gene mutations (left panel); and representing the highest 50% (grey) compared to lowest 50% (black) TRA CDR3 isoelectric points among barcodes that did not have any PIK3CA gene mutations (right panel). Median OS for the highest 50% isoelectric point group, in the PIK3CA mutated barcode set, 22.14 months. Median OS for lowest 50% isoelectric point group, in the PIK3CA mutated barcode set, 104.6 months. Log rank comparison *p* value 0.0287. Median OS for the highest 50% isoelectric point group in the barcodes set lacking PIK3CA mutations, 28.22 months. Median OS for the lowest 50% isoelectric point group in the barcode set lacking PIK3CA mutations, 44.28 months. Log rank comparison *p* value 0.0953. **b** KM analysis of DFS for BLCA barcodes representing the highest 50% (grey) compared to the lowest 50% (black) TRA CDR3 isoelectric points among barcodes representing PIK3CA gene mutations (left panel); and representing the highest 50% (grey) compared to the lowest 50% (black) TRA CDR3 isoelectric points among barcodes that did not have any PIK3CA gene mutations (right panel). Median DFS for the highest 50% isoelectric point group in the PIK3CA mutated barcode set, 20.37 months. Median DFS for lowest 50% isoelectric point group in the PIK3CA mutated barcode set, 101.4 months. Log rank comparison *p* value 0.0036. Median DFS for highest 50% isoelectric point group in the barcode set lacking PIK3CA mutations, 28.06 months. Median DFS for lowest 50% isoelectric point in the barcode set lacking PIK3CA mutations, 44.15 months. Log rank comparison *p* value 0.6423. **c** KM analysis of OS for BLCA barcodes representing the highest 50% (grey) compared to the lowest 50% (black) TRA CDR3 isoelectric points among the barcodes representing ITPR2 gene mutations (left panel); and representing the highest 50% (grey) compared to the lowest 50% (black) TRA CDR3 isoelectric points among barcodes that did not have any ITPR2 gene mutations (right panel). Median OS for highest 50% isoelectric point group in the ITPR2 mutated barcode set, 15.11 months. Median OS for lowest 50% isoelectric point group in the ITPR2 mutated barcode set, undefined. Log rank comparison *p* value 0.0052. Median OS for highest 50% isoelectric point group in the barcode set lacking ITPR2 mutations, 31.18 months. Median OS for lowest 50% isoelectric point group in the barcode set lacking ITPR2 mutations, 44.91 months. Log rank comparison *p* value 0.1961. **d** KM analysis of DFS for BLCA barcodes representing the highest 50% (grey) compared to lowest 50% (black) TRA CDR3 isoelectric points among the barcodes representing ITPR2 gene mutations (left panel); and representing the highest 50% (grey) compared to the lowest 50% (black) TRA CDR3 isoelectric points among barcodes that did not have any ITPR2 gene mutations (right panel). Median DFS for highest 50% isoelectric point group in the ITPR2 mutated barcode set, 20.37 months. Median DFS for lowest 50% isoelectric point in the ITPR2 mutated barcode set, undefined. Log rank comparison *p* value 0.0006. Median DFS for highest 50% isoelectric point group in the barcode set lacking ITPR2 mutations, 24.9 months. Median DFS for lowest 50% isoelectric point group in the barcode set lacking ITPR2 mutations, 51.41 months. Log rank comparison *p* value 0.1812

residues with a positive charge, and net charge per residue (NCPR) were calculated with the localCIDER python package (http://pappulab.github.io/localCIDER/). (TRA CDR3 physico-chemical features output, Table S3.)

Assessment of survival associations with TRA CDR3 chemical features

Survival correlations with TRA CDR3 physico-chemical features were performed by separating barcodes into top and bottom halves or quintiles based on each individual chemical feature, then performing a Kaplan–Meier (KM) survival analysis comparing the top and bottom groups, using GraphPad Prism software (version 7), which also outputted figures.

Assessment of survival associations for gene mutants and non-mutants overlapping TRA CDR3s with specific chemical features

Open-access Mutect gene mutation information was obtained from the GDC web portal (https://portal.gdc.cancer.gov/). Using an original script (available upon email to the corresponding author), barcodes were separated into mutant and non-mutant groups. Both groups were further separated by highest and lowest halves based on the quantification of particular physico-chemical properties. KM survival analyses were performed comparing highest versus lowest physico-chemical property barcode group, within a given gene mutation, barcode set; and by comparing highest versus lowest physico-chemical property barcode groups within a barcode set that lack mutations in the corresponding gene. These two KM analyses were performed for every physico-chemical property, for every gene for which mutation information was available, for both overall survival (OS) and disease-free survival (DFS). Genes for which an OS or DFS distinction based on a physico-chemical property was observed, among the patients also having a particular mutated gene, but not among the patients lacking a mutation in that gene, were further considered as indicated in "Results".

Results

To assess correlations between TCR CDR3 domain physico-chemical properties and survival we first performed V(D)J recombination read recovery on 418 TCGA BLCA primary tumor WXS files. CDR3 regions of the TRA recombination reads were translated into an AA sequence and analyzed first for isoelectric point.

Overall survival (OS) and disease-free survival (DFS) represented by barcodes representing the highest half of TRA CDR3 isoelectric points (Table S4) were compared to the barcodes representing the lowest half of isoelectric points using Kaplan–Meier (KM) survival analysis (Table 1). Note in particular that the isoelectric points, assessed as in "Methods", of the top and bottom fiftieth percentiles, were significantly different (Table 1). Barcodes

representing the lowest half of TRA CDR3 isoelectric points represented significantly increased OS ($n=112$, $p=0.027$) and DFS ($n=85$, $p=0.035$) compared to barcodes representing the highest half of isoelectric points, for the TRA CDR3s (Fig. 1). Similar analyses of the CDR3 domains represented by the TRB, TRG, TRD, IGH, IGK, and IGL recombination reads recovered from the bladder tumor tissue samples did not indicate any statistically significant survival associations. Also, no chemical features of the CDR3 domains represented by the TRA recombination reads recovered from bladder cancer patient blood WXS files correlated with survival distinctions.

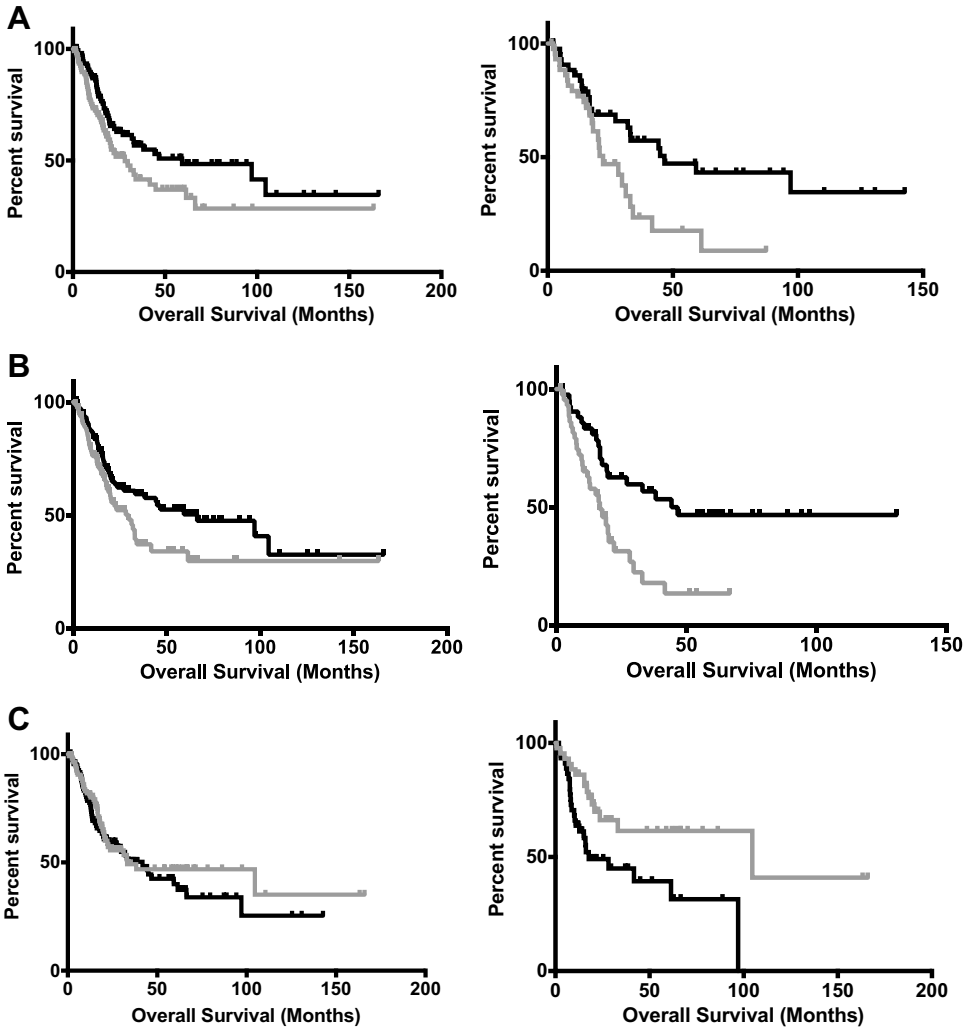

Fig. 3 Additional TRA CDR3 physico-chemical parameters distinguishing BLCA survival rates. **a** KM analysis of OS for BLCA barcodes representing the highest 50% (grey) compared to the lowest 50% (black) TRA CDR3 net charge per residue (NCPR) (left panel); and representing the highest 20% (grey) compared to lowest 20% (black) TRA CDR3 NCPR (right panel). Median OS for the highest 50% NCPR group, 28.22 months. Median OS for the lowest 50% NCPR group, 59.26 months. Log rank comparison p value, 0.0330. Median OS for the highest 20% NCPR group, 22.14 months. Median OS for the lowest 20% NCPR group, 46.65 months. Log rank comparison p value, 0.0111. **b** KM analysis of OS for BLCA barcodes representing the highest 50% (grey) compared to the lowest 50% (black) for the TRA CDR3 fraction of positive residues (left panel); and representing the highest 20% (grey) compared to the lowest 20% (black) (right) TRA CDR3 fraction of positive residues. Median OS for highest 50% fraction of positive residues group, 29.7 months. Median OS for lowest 50% fraction of positive residues group, 66.36 months. Log rank comparison p value, 0.0381. Median OS for highest 20% fraction of positive residues group, 16.69 months. Median OS for lowest 20% fraction of positive residues group, 44.28 months. Log rank comparison p value, 0.0014. **c** KM overall survival curves for BLCA barcodes representing the highest 50% (grey) compared to the lowest 50% (black) of TRA CDR3 fraction of tiny residues (left panel); and representing the highest 20% (grey) compared to lowest 20% (black) of TRA CDR3 fraction of tiny residues (right panel). Median OS for highest 50% fraction of tiny residues group, 33.11 months. Median OS for lowest 50% fraction of tiny residues group, 41.21 months. Log rank comparison p value, 0.4523. Median OS for highest 20% fraction of tiny residues group, 104.6 months. Median OS for lowest 20% fraction of tiny residues group, 17.71 months. Log rank comparison p value, 0.0079

To assess potential relationships between tumor-resident TRA CDR3 domain physico-chemical properties and mutant proteins in the tumor, we used Mutect mutation information obtained from the GDC. For each gene for which mutation data were available, we separated barcodes into mutated-gene and nonmutated-gene groups. These two groups were subdivided by highest and lowest, fiftieth percentile, TRA CDR3 isoelectric points. Two KM survival analyses were then performed. The first KM analysis compared the survival rates represented by the barcodes with gene mutations and the highest half of isoelectric point values for the TRA CDR3s, versus barcodes with mutations (in the same gene) and the lowest half of the isoelectric point values for the TRA CDR3s. A second KM analysis compared barcodes representing the lack of mutations for the same gene and with the highest half of isoelectric point values for the TRA

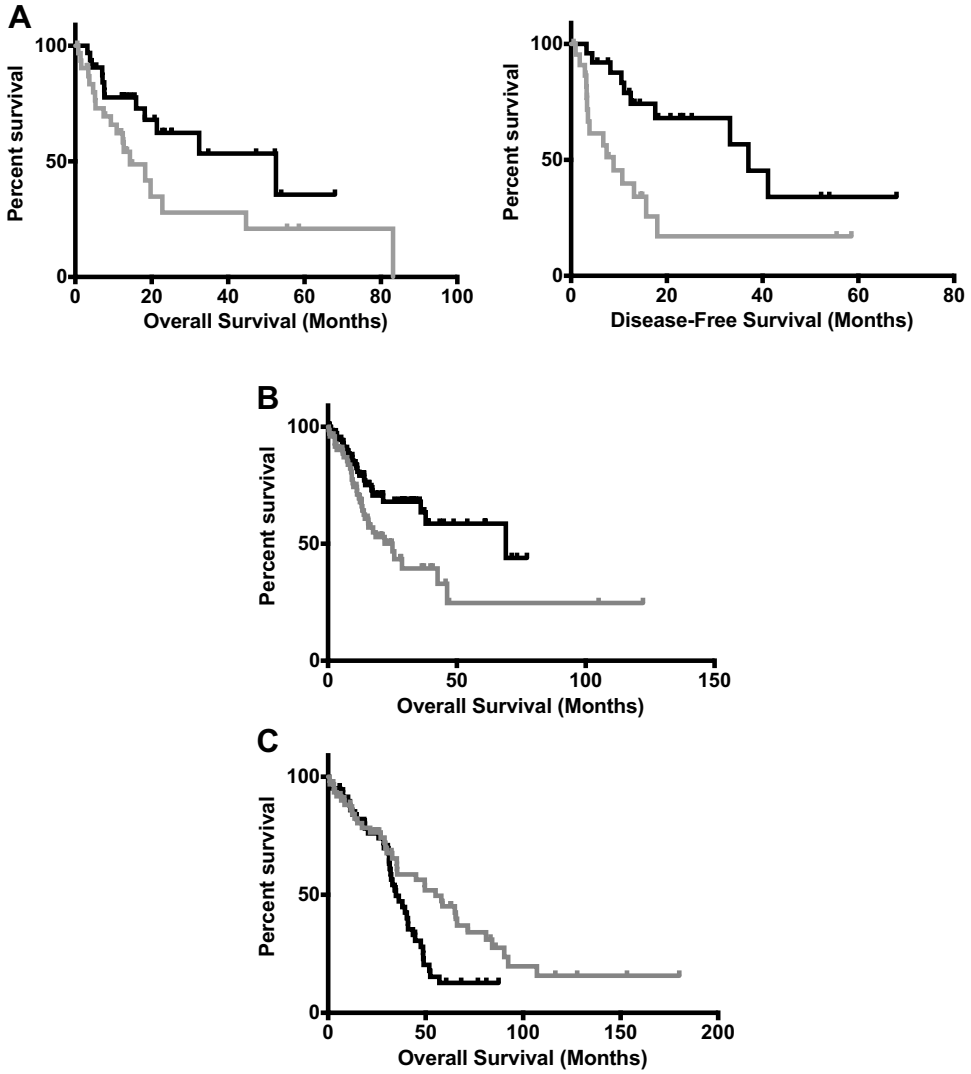

Fig. 4 TRA CDR3 physico-chemical properties distinguishing survival rates for additional cancers. **a** KM analysis of OS for ESCA barcodes representing the highest 50% (grey) compared to the lowest 50% (black) TRA CDR3 isoelectric points (left panel); and KM analysis of DFS for ESCA barcodes representing the highest 50% (grey) compared to the lowest 50% (black) of TRA CDR3 isoelectric points (right panel). Median OS for the highest 50% isoelectric point group, 14.29 months. Median OS for the lowest 50% isoelectric point group, 52.53 months. Log rank comparison *p* value, 0.0410. Median DFS for the highest 50% isoelectric point group, 8.87 months. Median DFS for the lowest 50% isoelectric point group, 37.42 months. Log rank comparison *p* value, 0.0043. **b** KM analysis of OS for STAD barcodes representing the highest 50% (grey) compared to the lowest 50% (black) of TRA CDR3 fraction of positive residues. Median OS for highest 50% fraction of positive residues group, 25.03 months. Median OS for lowest 50% fraction of positive residues, 68.99 months group. Log rank comparison *p* value, 0.0154. **c** KM analysis of OS for OVCA barcodes representing the highest 50% (grey) compared to the lowest 50% (black) TRA CDR3 fraction of positive residues. Median OS for the highest 50% fraction of positive residues group, 55.12 months. Median OS for lowest 50% fraction of positive residues group, 34.79 months. Log rank comparison *p* value 0.0147

CDR3s, versus barcodes lacking mutations but with the lowest half of TRA CDR3 isoelectric values.

Only several genes, out of a total of 14,256 mutated genes in the TCGA BLCA dataset, were identified whereby a low CDR3 isoelectric point value correlated with a significantly increased OS and DFS for the mutated gene barcode set but not for the non-mutated gene barcode set (Table 2). Interestingly, in 7 out of the 8 genes identified, the average change in isoelectric point, due to the mutant amino acid substitution, was positive, i.e., there was an apparent isoelectric point change in the mutant protein that was complementary to the TRA CDR3 isoelectric point group that represented the higher survival rate. The mutated genes that encoded the greatest (complementary) change in isoelectric point, PIK3CA and ITPR2 (Fig. 2) are commonly mutated in bladder cancer (Lopez-Knowles et al. 2006) (PIK3CA, 54 samples out of 227 samples with TRA read recovery from the BLCA WXS files; ITPR2, 26 out of 227).

To assess whether other physico-chemical properties of the TRA CDR3s, recovered from the BLCA WXS files, were correlated with survival rates, we performed similar analyses, dividing barcodes into top and bottom 50th percentiles by aromaticity, hydropathy, molecular weight, and charge. We found that lower net charge per residue (NCPR) ($n=112$, $p=0.033$), and fewer fraction of positive residues in the TRA CDR3 regions ($n=112$, $p=0.038$) also correlated with better OS (Fig. 3).

To determine whether the TRA CDR3 isoelectric point values, NCPR, or fraction of positive residues correlated with survival in other cancers, we repeated the above analyses on all TCGA cancer datasets. We found that low isoelectric point values and low NCPR were correlated with increased OS ($n=32$, $p=0.041$) and DFS ($n=24$, $p=0.0043$) in esophageal cancer (ESCA) (Fig. 4a). Moreover, the two ESCA barcode sets represented by these isoelectric point and NCPR survival distinctions, respectively, overlapped exactly. We also found that the fraction of positive residues was associated with low OS in stomach adenoma (STAD) ($n=78$, $p=0.0154$) (Fig. 4b), and better OS in ovarian cancer (OV) ($n=62$, $p=0.0147$) (Fig. 4c).

Discussion

Results of the above analysis are consistent with the idea that TILs with CDR3s with particular chemical features can be grouped to predict cancer survival rates. These results are also consistent with the idea that the common chemical features of the longer surviving BLCA patients may represent specific interactions with common antigens. For example, of the 14,256 BLCA mutants analyzed, only 8 reflected a survival distinction based on a distinct, complementary CDR3 chemical feature, namely the TRA CDR3, low isoelectric point group. And, 7 out of these 8 reflected a complementary isoelectric point. Thus, the approach of identifying CDR3 chemical features associated with survival may have the potential of identifying tumor antigens common to more than one patient. Such antigens may ultimately prove useful as vaccines or ways to increase ex-vivo stimulation of therapeutic TILs. And, given that common CDR3s should identify common antigens, such antigens may represent driver mutants, i.e., mutants appearing in numerous patients beyond what is expected by random chance. In the above analysis, ITPR2 mutants may represent just such an example, as these mutants have not been well studied in bladder cancer etiology.

Additional, unpublished analyses indicated that there were no correlations of either the mutant PIK3CA or HLA class I or class II alleles with low isoelectric point TRA CDR3s associated with survival (and capable of subdividing the BLCA mutants of Table 2 into distinct survival categories). This lack of a result allows no conclusions to be drawn, but it does raise the question of whether CDR3s with phyisco-chemical properties associated with survival pre-exist in the patient, as opposed to being stimulated by the cancer development?

Acknowledgements Authors wish to acknowledge the support of USF research computing and the taxpayers of the State of Florida.

Compliance with ethical standards

Conflict of interest Authors have nothing to declare.

Ethical approval This article does not contain any studies with human participants or animals performed by any of the authors.

References

Brown SD, Raeburn LA, Holt RA (2015) Profiling tissue-resident T cell repertoires by RNA sequencing. Genome Med 7:125

Callahan BM, Tong WL, Blanck G (2018a) T cell receptor-beta J usage, in combination with particular HLA class II alleles, correlates with better cancer survival rates. Immunol Res 66:219–223

Callahan BM, Yavorski JM, Tu YN, Tong WL, Kinskey JC, Clark KR, Fawcett TJ, Blanck G (2018b) T-cell receptor-beta V and J usage, in combination with particular HLA class I and class II alleles, correlates with cancer survival patterns. CII, Cancer immunology

Chen SA, Tsai MH, Wu FT, Hsiang A, Chen YL, Lei HY, Tzai TS, Leung HW, Jin YT, Hsieh CL, Hwang LH, Lai MD (2000) Induction of antitumor immunity with combination of HER2/neu DNA vaccine and interleukin 2 gene-modified tumor vaccine. Clin Cancer Res 6:4381–4388

Cheng L, Guo Y, Zhan S, Xia P, Association between HLA-DP gene polymorphisms and cervical cancer risk: a meta-analysis, Biomed Res Int, 2018 (2018) 7301595

Davila ML, Kloss CC, Gunset G, Sadelain M (2013) CD19 CAR-targeted T cells induce long-term remission and B Cell Aplasia in an immunocompetent mouse model of B cell acute lymphoblastic leukemia. PloS One 8:e61338

Di Sante G, Tolusso B, Fedele AL, Gremese E, Alivernini S, Nicolo C, Ria F, Ferraccioli G (2015) Collagen specific T-cell repertoire and HLA-DR alleles: biomarkers of active refractory rheumatoid arthritis. EBioMedicine 2:2037–2045

el-Demiry MI, Smith G, Ritchie AW, James K, Cumming JA, Hargreave TB, Chisholm GD (1987) Local immune responses after intravesical BCG treatment for carcinoma in situ. Br J Urol 60:543–548

Gill TR, Samy MD, Butler SN, Mauro JA, Sexton WJ, Blanck G (2016) Detection of productively rearranged TcR-alpha V-J sequences in TCGA exome files: implications for tumor immunoscoring and recovery of antitumor T-cells. Cancer Inf 15:23–28

Iglesia MD, Parker JS, Hoadley KA, Serody JS, Perou CM, Vincent BG (2016) Genomic analysis of immune cell infiltrates across 11 tumor types. J Natl Cancer Inst 108

Kinskey JC, Tu YN, Tong WL, Yavorski JM, Blanck G (2018) Recovery of immunoglobulin vj recombinations from pancreatic cancer exome files strongly correlates with reduced survival. Cancer Microenviron

Klarenbeek PL, Doorenspleet ME, Esveldt RE, van Schaik BD, Lardy N, van Kampen AH, Tak PP, Plenge RM, Baas F, de Bakker PI, de Vries N (2015) Somatic variation of T-cell receptor genes strongly associate with HLA class restriction. PloS One 10:e0140815

Kochenderfer JN, Dudley ME, Kassim SH, Somerville RP, Carpenter RO, Stetler-Stevenson M, Yang JC, Phan GQ, Hughes MS, Sherry RM, Raffeld M, Feldman S, Lu L, Li YF, Ngo LT, Goy A, Feldman T, Spaner DE, Wang ML, Chen CC, Kranick SM, Nath A, Nathan DA, Morton KE, Toomey MA, Rosenberg SA (2015) Chemotherapy-refractory diffuse large B-cell lymphoma and indolent B-cell malignancies can be effectively treated with autologous T cells expressing an anti-CD19 chimeric antigen receptor. J Clin Oncol 33:540–549

Li B, Li T, Pignon JC, Wang B, Wang J, Shukla SA, Dou R, Chen Q, Hodi FS, Choueiri TK, Wu C, Hacohen N, Signoretti S, Liu JS, Liu XS (2016) Landscape of tumor-infiltrating T cell repertoire of human cancers. Nature genetics 48:725–732

Li B, Li T, Wang B, Dou R, Zhang J, Liu JS, Liu XS (2017) Ultrasensitive detection of TCR hypervariable-region sequences in solid-tissue RNA-seq data. Nat Genet 49:482–483

Lopez-Knowles E, Hernandez S, Malats N, Kogevinas M, Lloreta J, Carrato A, Tardon A, Serra C, Real FX (2006) PIK3CA mutations are an early genetic alteration associated with FGFR3 mutations in superficial papillary bladder tumors. Cancer Res 66:7401–7404

Mai AT, Tong WL, Tu YN, Blanck G (2018) T-cell receptor-alpha recombinations in renal cell carcinoma exome files correlate with an intermediate level of T-cell exhaustion biomarkers, International immunology

Parodi A, Traverso P, Kalli F, Conteduca G, Tardito S, Curto M, Grillo F, Mastracci L, Bernardi C, Nasi G, Minaglia F, Simonato A, Carmignani G, Ferrera F, Fenoglio D, Filaci G (2016) Residual tumor micro-foci and overwhelming regulatory T lymphocyte infiltration are the causes of bladder cancer recurrence. Oncotarget 7:6424–6435

Prescott S, James K, Busuttil A, Hargreave TB, Chisholm GD, Smyth JF (1989) HLA-DR expression by high grade superficial bladder cancer treated with BCG. Br J Urol 63:264–269

Samy MD, Tong WL, Yavorski JM, Sexton WJ, Blanck G (2017) T cell receptor gene recombinations in human tumor specimen exome files: detection of T cell receptor-beta VDJ recombinations associates with a favorable oncologic outcome for bladder cancer. Cancer Immunol, Immunother 66:403–410

Stober U (1978) Influence of T-lymphocytes in bladder cancer on appearance and infiltration of recurrences (author's transl). Urologe A 17:296–302

Tong WL, Tu YN, Samy MD, Sexton WJ, Blanck G (2017) Identification of immunoglobulin V(D)J recombinations in solid tumor specimen exome files: evidence for high level B-cell infiltrates in breast cancer. Hum Vac Immunother 13:501–506

Tu YN, Tong WL, Samy MD, Yavorski JM, Kim M, Blanck G (2017a) Assessing microenvironment immunogenicity using tumor specimen exomes: co-detection of TcR-alpha/beta V(D)J recombinations correlates with PD-1 expression. J Int Cancer

Tu YN, Tong WL, Fawcett TJ, Blanck G (2017b) Lung tumor exome files with T-cell receptor recombinations: a mouse model of T-cell infiltrates reflecting mutation burdens. Lab Invest 97:1516–1520

Tu YN, Tong WL, Yavorski JM, Blanck G (2018) Immunogenomics: a negative prostate cancer outcome associated with TcR-gamma/delta recombinations. Cancer Microenviron

Zeng G, Huang Y, Huang Y, Lyu Z, Lesniak D, Randhawa P (2016) Antigen-specificity of T cell infiltrates in biopsies with T cell-mediated rejection and BK polyomavirus viremia: analysis by next generation sequencing. Am J Transpl 16:3131–3138